Active Brown Adipose Tissue Is Associated With a Healthier Metabolic Phenotype in Obesity

Carsten T. Herz,[1,2] Oana C. Kulterer,[1,3] Marlene Prager,[1] Christoph Schmöltzer,[1] Felix B. Langer,[4] Gerhard Prager,[4] Rodrig Marculescu,[5] Alexandra Kautzky-Willer,[1] Marcus Hacker,[3] Alexander R. Haug,[3] and Florian W. Kiefer[1]

Diabetes 2022;71:93–103 | https://doi.org/10.2337/db21-0475

Obesity is associated with increasing cardiometabolic morbidity and mortality rates worldwide. Not everyone with obesity, however, develops metabolic complications. Brown adipose tissue (BAT) has been suggested to be a promoter of leanness and metabolic health. To date, little is known about the prevalence and metabolic function of BAT in people with severe obesity, a population at high cardiometabolic risk. In this cross-sectional study, we included 40 individuals with World Health Organization class II-III obesity (BMI ≥35 kg/m^2). Using a 150-min personalized cooling protocol and ^{18}F-fluorodeoxyglucose (^{18}F-FDG) positron emission tomography/computed tomography, cold-activated BAT was detectable in 14 of the participants (35%). Cold-induced thermogenesis was significantly higher in participants with detectable BAT compared with those without. Notably, individuals with obesity and active BAT had 28.8% lower visceral fat mass despite slightly higher total fat mass compared with those without detectable BAT ^{18}F-FDG uptake. The lower amount of visceral fat mass was accompanied by lower insulin resistance and systemic inflammation and improved nonalcoholic fatty liver disease parameters, all adjusted for age, sex, and percent body fat. Contrary to previous assumptions, we show here that a significant fraction of individuals with severe obesity has active BAT. We found that decreased BAT ^{18}F-FDG uptake was not associated with adiposity per se but with higher visceral fat mass. In summary, active BAT is linked to a healthier metabolic phenotype in obesity.

The worldwide prevalence of overweight and obesity is at an all-time high. Obesity is associated with increased morbidity and mortality caused by higher rates of type 2 diabetes mellitus, dyslipidemia, hypertension, cardiovascular disease, obstructive sleep apnea syndrome, nonalcoholic fatty liver disease (NAFLD), and oncologic disease (1). The detrimental consequences of obesity, however, cannot be captured by body weight or percent body fat (%BF) alone. Central obesity, characterized by an increased visceral fat volume, is the determining factor for cardiometabolic morbidity and mortality, whereas the gynoid femoro-gluteal fat accumulation carries no such risk (2). In epidemiological studies, a metabolically healthy obese phenotype is defined by normal insulin sensitivity or the absence of components of the metabolic syndrome (3). It is not entirely clear, however, how this obese metabolic phenotype is determined.

In recent years, clinical research using ^{18}F-fluorodeoxyglucose (^{18}F-FDG) positron emission tomography/computed tomography (PET/CT) imaging demonstrated that brown adipose tissue (BAT) is still active in adults and is inversely associated with obesity (4–8). BAT can be activated through cold exposure, which results in enhanced

[1]Division of Endocrinology and Metabolism, Department of Medicine III, Medical University of Vienna, Vienna, Austria
[2]Division of Nephrology and Dialysis, Department of Medicine III, Medical University of Vienna, Vienna, Austria
[3]Division of Nuclear Medicine, Department of Biomedical Imaging and Image-Guided Therapy, Medical University of Vienna, Vienna, Austria
[4]Division of General Surgery, Department of Surgery, Medical University of Vienna, Vienna, Austria
[5]Division of Medical-Chemical Laboratory Diagnostics, Department of Laboratory Medicine, Medical University of Vienna, Vienna, Austria

Corresponding author: Florian W. Kiefer, florian.kiefer@meduniwien.ac.at

Received 27 May 2021 and accepted 13 October 2021

This article contains supplementary material online at https://doi.org/10.2337/figshare.16811086

glucose uptake that can be quantified using PET/CT scans. BAT depots are characterized by adipocytes with a high density in mitochondria and multilocular lipid droplets. When activated via the β-adrenergic pathway, mitochondrial respiration is uncoupled from ATP synthesis by uncoupling protein-1, a tissue-specific protein found in the inner mitochondrial membrane. By releasing protons in the mitochondrial matrix, uncoupling protein-1 dissipates chemical energy as heat, a process termed *nonshivering thermogenesis* (9). Accumulating evidence shows that cold-induced BAT activity is associated with enhanced energy expenditure in humans (4,8,10). We have recently demonstrated that lean individuals with active BAT (BAT_{pos}) burn significantly more calories during cold conditions and have a favorable oxylipin profile compared with those without detectable BAT (BAT_{neg}) (11). However, it has been suggested that the presence and activity of BAT are declining with age and the degree of adiposity (12). In small clinical studies, intermittent cold acclimation for 10 days up to 6 weeks led to a recruitment of active BAT, which was paralleled by improvements in body fat percentage and glucose metabolism (8,13,14), suggesting that promotion of BAT mass and activity may be a promising intervention to counteract obesity-related metabolic complications. Yet, most BAT research in humans has focused on healthy, predominantly male, normal weight to moderately overweight individuals, neglecting the group at the highest risk for obesity-related adverse outcomes. Hence, the aim of this study was to investigate the prevalence of cold-activated BAT and the metabolic phenotype associated with the presence of active BAT in a unique cohort of World Health Organization (WHO) class II-III obese individuals.

RESEARCH DESIGN AND METHODS

Study Participants

Forty participants with WHO class II-III obesity (BMI ≥35 m/kg^2) were recruited between 2017 and 2019 at the Department of Surgery of Vienna General Hospital for a longitudinal study investigating the impact of bariatric surgery on BAT activity. The study visits were conducted in the cool season (between fall and spring) to avoid any seasonal influence on BAT activity. The study was approved by the Ethics Committee of the Medical University of Vienna (no. 1071/2017), and all participants provided written informed consent prior to enrollment in the study. Inclusion criteria were an age between 20 and 50 years and a BMI from 35 to 55 kg/m^2. Exclusion criteria included endocrine disease except for substituted hypothyroidism, chronic kidney disease, chronic liver disease, chronic inflammatory conditions requiring systemic therapies, as well as the use of medications modifying adrenergic receptor signaling.

Study Procedures

The participants were instructed to ingest an isocaloric diet and refrain from strenuous physical exercise during the 2 days before the study visit. They were further advised not to smoke after midnight and not to drink caffeine after 12 A.M. the day before the study visit. After an overnight fast (>10 h), the participants arrived between 7 A.M. and 8 A.M. at the institution's metabolic unit, where anthropomorphic measurements were performed. Waist circumference was measured at the midpoint between the lower border of the rib cage and the iliac crest, and hip circumference was measured around the widest portion of the hips. Height was measured using a stadiometer. Body composition, including body weight, was analyzed on a scale incorporating bio-electrical impedance analysis (seca mBCA 515; seca GmbH & Co., Hamburg, Germany) and by air displacement plethysmography (Bod Pod; COSMED, Rome, Italy). The percentage of body fat was calculated using a three-compartment model incorporating body density and total body water as estimated by the manufacturer's proprietary algorithm (15,16). Between 8 A.M. and 9 A.M., study participants rested in a supine position for 30 min before resting energy expenditure was measured for 30 min by indirect calorimetry using a canopy hood (Quark RMR; COSMED).

Gas and volume calibration of the metabolic cart were performed once at the beginning of each study day according to the manufacturer's instructions. After indirect calorimetry, blood samples were drawn from the indwelling catheter in an antecubital vein and processed immediately. Between 9 and 10 A.M., the participants were fitted with a water-perfused cooling vest that covered the whole torso (CoolShirt Systems, Stockbridge, GA). The temperature was gradually decreased until shivering was detected by electromyography (EMG; EMG Quattro; OT Bioeletronica, Torino, Italy) or the participant reported shivering or severe thermal discomfort. EMG electrodes were placed on the major pectoral muscle. Shivering was assessed in real-time always by the same study personnel and identified by sudden increases in the amplitude of the EMG signal either continuously or in bursts that were not attributable to voluntary muscle contractions. At any signs of shivering, the temperature of the cooling vest was increased by 1.12–2.24°C, and we re-evaluated whether additional temperature changes were necessary within 5–10 min. Some participants did not show shivering on the electromyelogram nor did they explicitly report they were shivering while they were experiencing severe thermal discomfort. In these cases, we also adjusted the temperature as described. The participants remained in a supine position throughout the whole cooling period. Between 10 A.M. and 11:30 A.M., during minutes 60–90 of the cooling protocol, a second indirect calorimetry was performed to assess cold-induced thermogenesis (CIT), which is expressed as the percent increase in energy expenditure after cold exposure as compared with baseline. Of the 30-min readings, the first 5 min were discarded; subsequently, the 5-min interval with the lowest combined coefficients of variation for VO_2 and VCO_2 were selected for the determination of energy expenditure, using the Weir formula. In a

previous study, this approach resulted in the lowest intra-individual variation, compared with other methods (17).

On study day 2, a mixed-meal tolerance test was performed. After an overnight fast, a baseline blood sample was collected from the participants between 7 A.M. and 9 A.M., shortly (1–3 min) before they ingested a high-caloric liquid meal (Nestlé Resource Energy, Vevey, Switzerland) containing ∼303 kcal (55% carbohydrates, 30% lipids, and 15% protein) within 5 min. Consecutively, blood samples were collected at minutes 15, 30, 60, 120, and 180 for the determination of glucose and insulin levels.

All laboratory analyses were performed using routine diagnostic assays at the institution's Department of Laboratory Medicine. For the determination of norepinephrine levels, blood samples were collected into chilled collecting tubes coated with glutathione and ethylene glycol tetraacetic acid. Quantification was performed by high-pressure liquid chromatography with a reported coefficient of variation of 8%–11%. EDTA plasma was stored at −80°C for the determination of fibroblast growth factor-21 (FGF-21) in duplicate, using a commercially available assay (Human FGF-21 Quantikine ELISA Kit; R&D Systems, Minneapolis, MN). The index of nonalcoholic steatohepatitis (NASH), the HOMA of insulin resistance (HOMA-IR) index, and the Matsuda insulin sensitivity index were calculated according to the published equations (18–20). Prediabetes was defined by a fasting glucose level between 100 and 125 mg/dL or an HbA_{1c} between 5.7% and 6.4% (21).

Weather data were retrieved online from *Zentralanstalt für Meteorologie und Geodynamik*, the national meteorological and geophysical service of Austria (https://www.zamg.ac.at/cms/de/klima/klimauebersichten/jahrbuch). We used the provided outdoor temperatures in Vienna, recorded at 7 A.M., 2 P.M., and 7 P.M., to calculate mean daytime outdoor temperature between 7 A.M. and 7 P.M. by the trapezoidal rule.

^{18}F-FDG PET/CT Imaging

After the second indirect calorimetry, between 10:30 A.M. and 11:30 A.M., 2.5 MBq/kg body weight of ^{18}F-FDG was administered intravenously followed by another 60 min of mild cold exposure during the accumulation time of the radiotracer, resulting in a total cooling period of 150 min. Then, a combined static PET/CT acquisition was started on a Siemens Biograph 64 Ture Point Scanner (Siemens Healthcare Sector, Erlangen, Germany). First, a low-dose CT scan was performed (120 kV, 50 mAs) for attenuation and scatter correction as well as for the anatomic localization of the BAT depots. PET acquisition was performed in three-dimensional mode with 3 min/bed position (n = 5 bed positions). The images were acquired from the base of the skull to midthigh.

Image Analysis

BAT ^{18}F-FDG uptake was quantified using the Hermes Hybrid 3D Viewer (Hermes Medical Solutions, Stockholm, Sweden). The regions of interest were delineated in the axial fusion images using a semiautomatically segmentation protocol in accordance with the Brown Adipose Reporting Criteria in Imaging Studies criteria (22). Briefly, only regions of interest located within a CT radio density of −190 to −10 HU and with a minimal standardized uptake value (SUV) higher than a personalized threshold of 1.2 divided by relative lean body mass were classified as active BAT. The resulting individualized SUV thresholds were in the range of 2.04 to 2.77. Two experienced nuclear medicine physicians visually inspected each slice to exclude spillover from adjacent nonfat tissues prone to ^{18}F-FDG uptake, such as muscles, glands, or lymph nodes. Detectable BAT volumes ranged from 21 to 383 mL. Participants with detectable BAT were categorized as BAT_{pos}.

Abdominal adipose tissue was delineated by placing a volume of interest (VOI) within fat radiodensity (−300 to −10 HU) on the low-dose CT along the level of the third lumbar vertebrae. Fat located underneath the skin and external to the abdominal and back muscles was identified as the subcutaneous compartment of white adipose tissue (SAT). Visceral adipose tissue (VAT), the adipose tissue located around the internal organs, was obtained by subtracting the amount of SAT from the entire fat depot.

Liver ^{18}F-FDG uptake was determined by placing one 8-cm^3 VOI in the right and one in the left liver lobe of each participant. The VOIs were placed ∼2 cm below the liver capsule to avoid large vessels. The ^{18}F-FDG blood-pool uptake was obtained by measuring the mean SUV (SUV_{mean}) of three different slices of the vena cava inferior. The target-to-background ratio (TBR) of the liver was calculated by dividing the peak SUV (SUV_{peak}) of the two liver VOIs to the mean SUV_{mean} within the vena cava inferior. Skeletal muscle ^{18}F-FDG uptake in triceps brachii, erector spinae on the level of vertebral body L4, and in gluteus maximus was quantified as previously described (23).

Statistics

The data are presented as counts, median (25th–75th percentile) or mean ± SD, as appropriate. Accordingly, between-group differences were tested using Student t test, Mann-Whitney U test, or χ^2 test. To investigate associations between two continuous variables, the Spearman rank correlation coefficient was used. Unadjusted and adjusted linear models were used to examine the associations between BAT status as the main independent variable and individual metabolic parameters as dependent variables. All analyses were presented unadjusted as well as adjusted for the confounding variables age, sex, %BF, VAT, HOMA-IR, and outdoor temperature. The regression coefficients are presented as standardized regression coefficients (β), meaning a 1-unit change of a continuous variable corresponds to a change by 1 SD of the respective variable.

All analyses were performed using SPSS 25 (IBM Corp., Armonk, NY) and GraphPad Prism 6.0 (GraphPad

Software Inc., La Jolla, CA). Two-sided *P* values ≤0.05 were deemed statistically significant.

Data and Resource Availability

The data sets generated and/or analyzed during this study are available from the corresponding author on reasonable request.

RESULTS

Active BAT Was Present in 35% of Individuals With Severe Obesity

In total, 40 participants (*n* = 32 women, *n* = 8 men) with WHO class II-III obesity were enrolled in this observational study: 10 with a BMI ≥35 and <40 kg/m^2 and 30 with a BMI ≥40 m/kg^2. Of the 40 participants, 31 were euglycemic and 9 were prediabetic according to fasting glucose or HbA_{1c} criteria. Upon cold stimulation, 14 participants (35%) were BAT_{pos}, as evidenced by ^{18}F-FDG uptake in the archetypical fat depots, whereas 26 individuals (65%) were BAT_{neg} (Fig. 1*A* and Table 1). Both groups were of similar age, whereas BAT_{pos} participants were exclusively female. BAT_{pos} participants had a lower BMI. There was no difference in blood pressure, circulating lipids, thyroid function (Table 1), or the adrenergic response to cooling; there were similar median cold-induced increases in norepinephrine levels in BAT_{pos} and BAT_{neg} individuals (Supplementary Fig. 1*A*). The temperatures of the water-perfusing cooling vests also did not differ between the two groups (Supplementary Fig. 1*B*).

Individuals With Obesity and Active BAT Had Higher CIT

After adjusting for lean body mass and fat mass, the resting energy expenditure was similar in BAT_{neg} and BAT_{pos} participants (Table 1). However, upon cold stimulation, the relative increase in CIT was significantly higher in BAT_{pos} than BAT_{neg} individuals (Fig. 1*B*). There were no differences in triceps brachii, erector spinae, and gluteus maximus ^{18}F-FDG uptake (Supplementary Fig. 2*A*–*C*). CIT correlated positively with BAT SUV_{mean} and BAT volume (Fig. 1*C* and *D*) but not with triceps brachii, erector spinae, and gluteus maximus ^{18}F-FDG SUV_{mean} (Supplementary Fig. 2*D*–*F*).

BAT_{pos} Individuals With Obesity Had Lower Visceral Fat Mass and Higher Insulin Sensitivity

Participants with cold-activated BAT had a lower waist-to-hip ratio and BMI, whereas %BF was higher than in BAT_{neg} participants (Fig. 2*A* and Table 1). To further dissect the relationship between BAT status and abdominal obesity, we analyzed the abdominal fat distribution at the level of vertebral body L3. Although total abdominal fat and VAT volume were significantly lower in BAT_{pos}

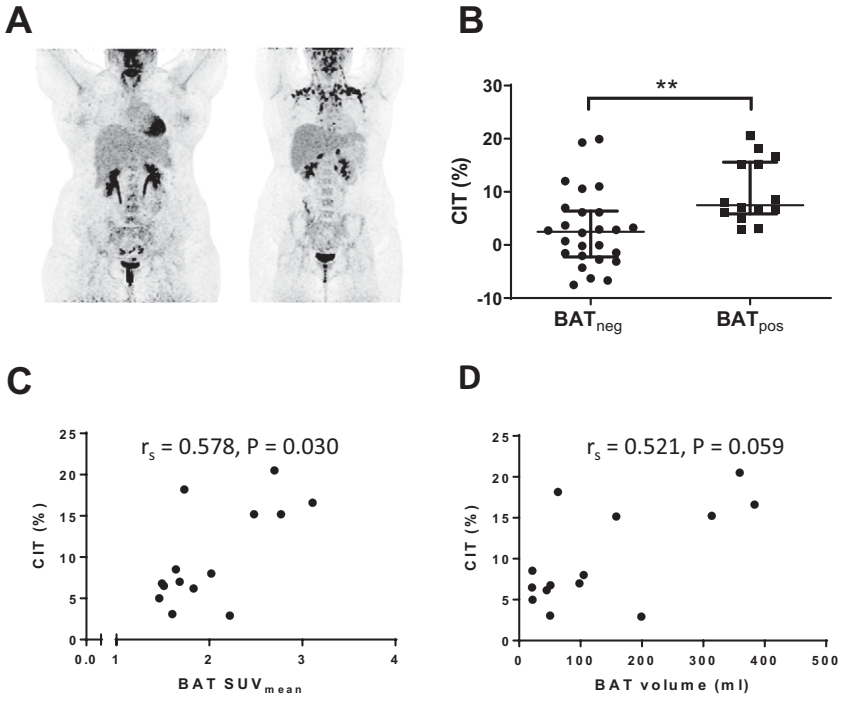

Figure 1—Active BAT is associated with increased energy expenditure in individuals with obesity. Representative PET images of a BAT_{neg} (left) and a BAT_{pos} (right) participant (*A*). Differences in CIT between BAT_{neg} and BAT_{pos} participants (*B*). The central bar shows the median value and the whisker indicates the interquartile range. Scatterplot for the positive association between CIT and SUV_{mean} in BAT (*C*). Scatterplot for the positive association between CIT and BAT volume (*D*). r_s, Spearman rank correlation coefficient. *$P \leq 0.050$, **$P \leq 0.010$, ***$P \leq 0.001$.

Table 1—Baseline characteristics of the study participants stratified by BAT status

	BAT_{neg} (n = 26)	BAT_{pos} (n = 14)	P
Age (years)	31 ± 9	31 ± 7	0.692
Sex, female, n (%)	18 (69.2)	14 (100)	0.034
BMI (kg/m^2)	44.7 ± 5	41.5 ± 3.3	0.037
BF (%)	50.1 ± 4.2	52.6 ± 2.3	0.022
Systolic BP (mmHg)	129 ± 13	124 ± 9	0.165
Diastolic BP (mmHg)	82 ± 12	80 ± 7	0.645
RMR (95% CI), kcal/day*	1,920 (1,836–2,006)	1,972 (1,850–2,095)	0.523
Triglycerides (mmol/L)	1.19 (0.8–1.52)	1.06 (0.7–1.21)	0.287
Cholesterol (mmol/L)	4.6 ± 0.98	4.49 ± 0.53	0.694
HDL-C (mmol/L)	1.15 ± 0.35	1.29 ± 0.31	0.205
LDL-C (mmol/L)	2.81 ± 0.71	2.61 ± 0.43	0.343
TSH (μU/mL)	2.53 ± 1.82	1.72 ± 1.12	0.139
fT4 (ng/dL)	1.17 ± 0.18	1.19 ± 0.15	0.759
HbA_{1c} (mmol/mol)	36.2 ± 4	33.5 ± 2.7	0.028
HbA_{1c} (%)	5.5 ± 0.4	5.2 ± 0.2	–
Glucose (mmol/L)	5.07 ± 0.53	4.86 ± 0.35	0.199
Insulin (μU/mL)	21 (16–31)	13 (11–19)	0.011
HOMA-IR	4.7 (3.4–7)	2.9 (2.1–4.1)	0.012
Matsuda index	2.2 (1.4–3.3)	3.7 (2.4–5)	0.015
Outdoor temperature (°C)	14.4 ± 8.2	9.5 ± 9.9	0.102

Data are reported as counts, mean ± SD, or median (interquartile range), as appropriate, unless otherwise indicated. BP, blood pressure; fT4, free thyroxine; HDL-C, high-density lipoprotein cholesterol; LDL-C, low-density lipoprotein cholesterol; RMR, resting metabolic rate; TSH, thyroid-stimulating hormone. *Estimated marginal mean values were adjusted for fat mass and lean body mass. –, not done.

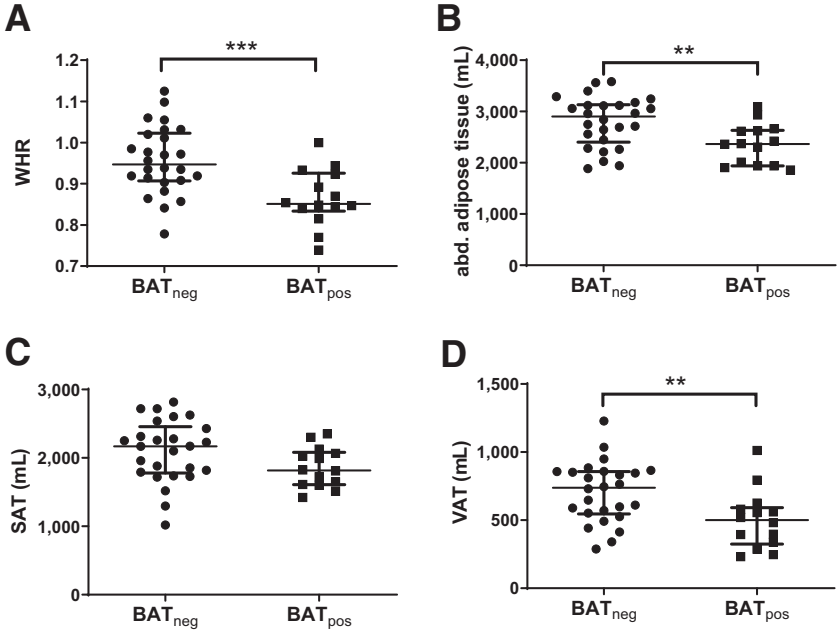

Figure 2—BAT_{pos} individuals with obesity have lower abdominal fat mass. Differences in waist-to-hip ratio (WHR) (*A*), total abdominal fat (*B*), abdominal SAT (*C*), and abdominal VAT (*D*) between BAT_{neg} and BAT_{pos} individuals. *$P \leq 0.050$, **$P \leq 0.010$, ***$P \leq 0.001$.

participants than in BAT_{neg} participants, the difference for SAT was weaker and not statistically significant (Fig. 2*B–D*). Because sex influences body composition and all BAT_{pos} participants were female, we performed analyses on data from women only. The differences in waist-to-hip ratio, VAT, and total abdominal fat remained statistically significant between $BAT_{neg\ and}$ BAT_{pos} participants (Supplementary Fig. 3*A–C*).

In rank correlation analysis, VAT showed strong inverse associations with CIT, BAT volume, and BAT SUV_{mean}, whereas SAT did not correlate with these parameters in the whole study group and in women only (Fig. 3 and Supplementary Fig. 3*E* and *F*). These data suggest that BAT activity is not associated with adiposity per se but with a distinct fat distribution in obesity favoring a gynoid femoro-gluteal phenotype.

Next, we studied if the beneficial relationship between BAT and visceral adiposity translated to a healthier metabolic phenotype. The presence of BAT was associated with increased insulin sensitivity, as indicated by a significantly lower HOMA-IR index and a higher Matsuda index after adjustment for age, sex, and %BF, or outdoor temperature in all participants and in women, respectively (Table 2 and Supplementary Table 1). However, adjusting for VAT weakened the associations between BAT and HOMA-IR as well as Matsuda index (Table 2 and Supplementary Table 1). The glycemic long-term marker HbA_{1c} was significantly lower in BAT_{pos} individuals (Table 2 and Supplementary Table 1). Only 1 of 14 participants (7%) in the BAT_{pos} group, compared with 8 of 26 participants (31%) in the BAT_{neg} group, had prediabetes (Fisher exact test P = 0.124). Lipid metabolism did not differ between BAT_{neg} and BAT_{pos} participants, as indicated by unaltered triglyceride, total cholesterol, LDL cholesterol, or HDL cholesterol levels (Table 2 and Supplementary Table 1). In summary, these data suggest the presence of active BAT is linked to lower insulin resistance and improved glucose metabolism in obesity.

Active BAT Was Associated With Advantageous NAFLD Parameters and Reduced Inflammation in Obesity

Given that obesity is frequently linked to NAFLD and systemic inflammation, we investigated the relationship between BAT and metabolic liver disease. Levels of the systemic inflammatory marker interleukin 6 and the early fatty liver marker γ-glutamyltransferase were significantly lower in BAT_{pos} individuals than BAT_{neg} individuals after we adjusted for age, sex, and %BF, or outdoor temperature, whereas adjustment for VAT or HOMA-IR mitigated these associations (Table 2 and Supplementary Table 1, Fig. 4*A* and *B* and Supplementary Fig. 4*A* and *B*). Levels of aspartate aminotransaminase, but not alanine aminotransferase (ALAT) were decreased in

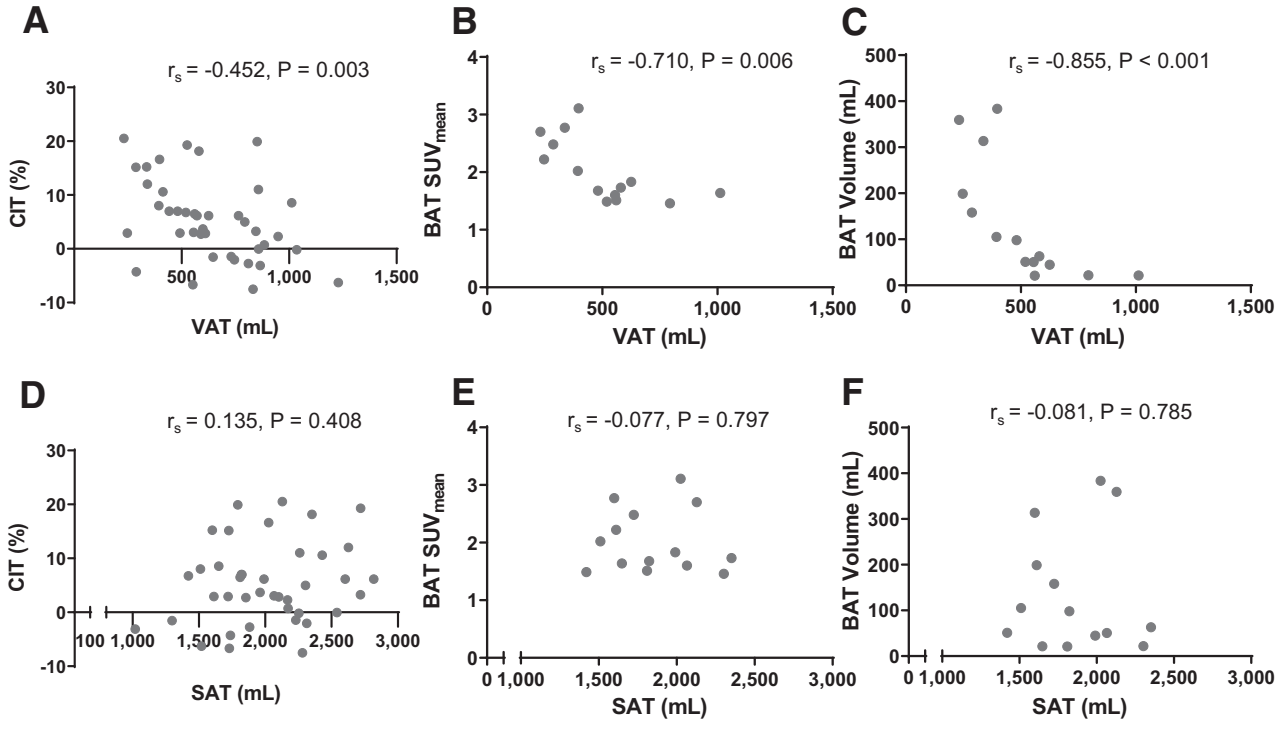

Figure 3—VAT but not SAT volume is inversely associated with BAT function. Scatterplots for the associations between VAT volume and CIT (*A*), BAT glucose uptake (SUV_{mean}) (*B*), as well as BAT volume (*C*). *D–F* show the same associations for abdominal SAT. r_s, Spearman rank correlation coefficient. *$P \leq 0.050$, **$P \leq 0.010$, ***$P \leq 0.001$.

Table 2—Differences in metabolic parameters between all BAT_{neg} and BAT_{pos} participants

	Model no.											
	1: Unadjusted		2: Adjusted for age and sex		3: Adjusted for age, sex, and %BF		4: Adjusted for age, sex, and VAT		5: Adjusted for age, sex, and HOMA-IR		6: Adjusted for age, sex, and outdoor temperature	
	β	*P*	β	*P*	β	*P*	β	*P*	β	*P*	β	*P*
HOMA-IR*	−0.918	0.004	−0.988	0.007	−0.996	0.007	−0.648	0.058	–	–	−0.972	0.014
Matsuda index*	0.937	0.011	0.911	0.031	0.923	0.030	0.483	0.229	–	–	0.902	0.044
HbA_{1c}	−0.706	0.032	−0.879	0.018	−0.873	0.020	−0.779	0.050	−0.233	0.487	0.0.969	0.015
TG*	−0.317	0.346	−0.226	0.554	−0.207	0.592	−0.003	0.994	−0.084	0.844	−0.240	0.564
Cholesterol	−0.133	0.694	0.062	0.870	0.092	0.808	0.019	0.962	−0.152	0.716	0.011	0.979
HDL-C	0.424	0.205	0.353	0.335	0.334	0.366	0.059	0.871	0.031	0.936	0.315	0.427
LDL-C	−0.319	0.343	−0.059	0.873	−0.014	0.970	−0.084	0.835	−0.235	0.569	−0.120	0.766
CRP*	−0.347	0.301	−0.477	0.208	−0.514	0.170	−0.406	0.316	−0.186	0.647	−0.727	0.069
IL-6*	−0.742	0.027	−0.819	0.022	−0.862	0.009	−0.683	0.066	−0.654	0.091	−0.871	0.026
GGT*	−1.068	0.001	−0.880	0.011	−0.889	0.011	−0.657	0.054	−0.584	0.106	−1.120	0.003
ALAT*	−0.489	0.142	−0.237	0.504	−0.231	0.521	−0.007	0.984	0.031	0.935	−0.314	0.414
ASAT*	−0.770	0.021	−0.726	0.051	−0.709	0.060	−0.646	0.101	−0.815	0.052	−0.856	0.039
ION	−0.915	0.004	−0.965	0.008	−0.969	0.009	−0.600	0.074	0.003	0.967	−0.958	0.015
Liver TBR	−0.746	0.022	−0.708	0.055	−0.695	0.062	−0.609	0.120	−0.553	0.172	−0.586	0.135

ASAT, aspartate aminotransferase; CRP, C-reactive protein; GGT, γ-glutamyltransferase; HDL-C, high-density lipoprotein cholesterol; IL-6, interleukin 6; ION, index of nonalcoholic steatohepatitis; TG, triglyceride. *Log-transformed. The regression coefficients (β) depict the effect of the independent variable BAT status (BAT_{neg} = 0, BAT_{pos} = 1) on each metabolic parameter as the dependent variable. The dependent variables were entered as standardized *z*-scores. –, not done.

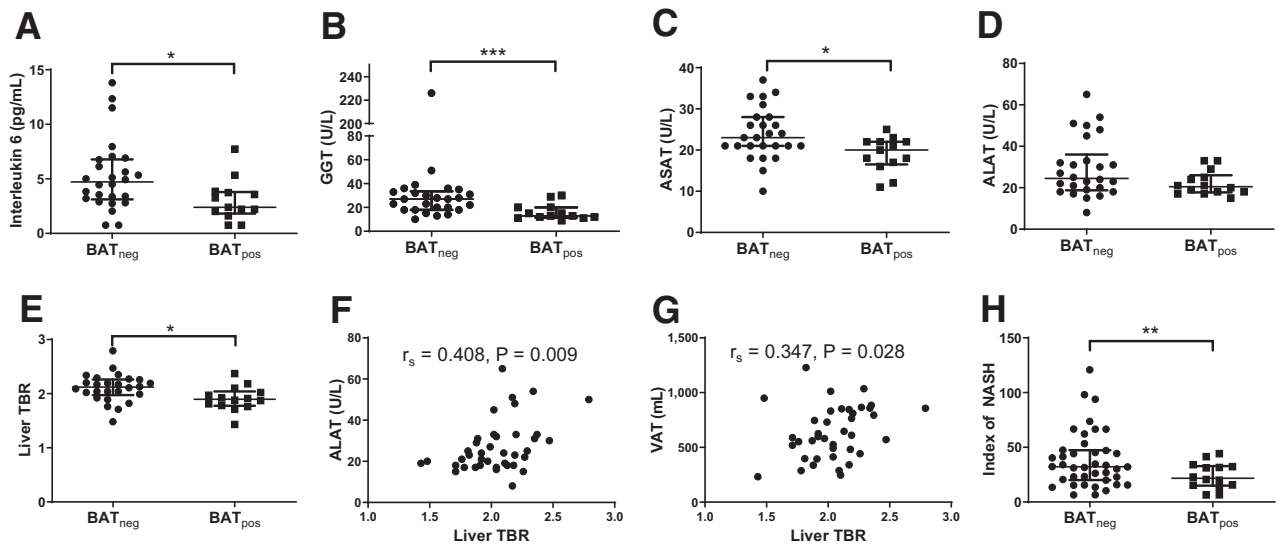

Figure 4—Active BAT is associated with improved NAFLD parameters and reduced inflammation. Dot plots for the comparison of interleukin 6 (IL-6) (*A*), γ-glutamyltransferase (GGT) (*B*), aspartate aminotransferase (ASAT) (*C*), and ALAT (*D*) levels; liver TBR (*E*); and index of NASH (*H*). The scatterplots depict the associations between liver TBR and ALAT (*F*) as well as between liver TBR and VAT (*G*). *$P \leq 0.050$, **$P \leq 0.010$, ***$P \leq 0.001$.

BAT$_{pos}$ individuals compared with BAT$_{neg}$ individuals (Table 2 and Supplementary Table 1, Fig. 4*C* and *D* and Supplementary Fig. 4*C* and *D*).

Liver glucose uptake has been proposed to be a marker for hepatic inflammation (24). Notably, liver ^{18}F-FDG uptake (liver TBR), as determined by PET scans, was significantly lower in BAT$_{pos}$ participants (Fig. 4*E* and Supplementary Fig. 4*E*; Table 2 and Supplementary Table 1), which was slightly attenuated after adjustment for age, sex, and %BF, VAT, HOMA-IR, or outdoor temperature. Liver TBR correlated positively with ALAT levels and VAT (Fig. 4*F* and *G* and Supplementary Fig. 4*F* and *G*). In line with these results, the index of NASH, a validated tool for the diagnosis of biopsy-proven NASH, was significantly lower in BAT$_{pos}$ individuals than in BAT$_{neg}$ individuals (Fig. 4*H* and Supplementary Fig. 4*H*; Table 2 and Supplementary Table 1). Levels of circulating FGF-21, a potential BATokine with effects on metabolic liver disease (25), did not differ between groups nor was FGF-21 associated with markers of BAT activity (Supplementary Fig. 5). An important question that often arises in the context of BAT studies like this is whether improved insulin sensitivity may bias BAT glucose uptake and other metabolic parameters. Therefore, we also compared individuals with similar HOMA-IR values, which yielded 10 matched women in each group (Supplementary Fig. 6). BAT$_{pos}$ individuals had still higher CIT, lower visceral fat mass, and improved liver function parameters (Supplementary Table 2), suggesting that the presence of active BAT may also have some positive metabolic effects independent of insulin resistance. Together, these findings suggest the presence of active BAT could be linked to a beneficial role in NAFLD in obese conditions.

DISCUSSION

Presence of Active BAT in Obesity

To our knowledge, this is the first study investigating the relationship between metabolic complications and cold-stimulated BAT in individuals with severe obesity (WHO class II-III), who bear the highest metabolic risk. Contrary to the notion that obesity is a state of BAT depletion, we found active BAT in 35% of the participants. This is a larger proportion than reported previously in a smaller study cohort, in which 3 of 15 individuals with morbid obesity had active BAT (26). Our findings are in accordance with those of two other studies in slightly leaner but still obese cohorts with mean BMI values of 34 and 35.4 kg/m^2 (7,27). In these studies, the proportions of BAT$_{pos}$ individuals were 31% and 43% (7,27). Most recently, BAT volume and radiodensity were found to be positively associated with adiposity in young overweight men, also challenging the previously believed concept that BAT is negatively associated with obesity (28), which was mainly based on PET studies at thermoneutrality instead of individualized cooling strategies. Nonetheless, the reported percentage of BAT positivity in obesity is still less than in young lean individuals, with some studies reporting BAT ^{18}F-FDG uptake in 40%–100% (4,12,29),

One of the most important questions in the context of clinical BAT research is whether the presence or recruitment of active BAT improves metabolic function in obesity. In previous studies, researchers have mainly investigated associations between BAT activity and body fat or energy metabolism in lean or slightly overweight individuals (6,7,10,12,26,30). Here, we characterized the metabolic differences between the presence or absence of BAT in individuals with class II-III obesity and

came to the conclusion that active BAT is tightly linked to a metabolically healthier obese phenotype characterized by higher insulin sensitivity, less visceral obesity, lower systemic inflammation, and more favorable liver parameters.

We show that BAT_{pos} individuals with obesity had a significantly higher cold-induced energy expenditure than BAT_{neg} individuals, comparable to lean populations (10,11). These findings suggest that despite severe adiposity, BAT might still be functional in obese individuals.

Active BAT Was Associated With Reduced Visceral Obesity and Healthier Glucose Metabolism

Results of previous studies suggested a strong negative association between BAT activity and BMI or body fat across lean and obese individuals (6,12,26). We demonstrated in the present report that in obesity, BAT glucose uptake was neither related to BMI nor %BF per se but to visceral fat accumulation (Fig. 2, Table 2, and Supplementary Table 1). Given that women have less visceral obesity and all participants in the BAT_{pos} group were female, we additionally performed our analyses in women only, which showed that the association between visceral obesity and BAT was not confounded by sex (Supplementary Fig. 3). In accordance with reduced VAT volume, BAT_{pos} individuals had less insulin resistance, lower HbA_{1c}, and were less likely to have prediabetes despite a pathologically increased total fat mass and BMI (Tables 1 and 2, and Supplementary Table 1). Although adjusting the associations between BAT and metabolic parameters for VAT weakened the associations (Table 2 and Supplementary Table 1), the resulting parameter estimates for the relevant variables still corresponded to a medium to large effect size (Cohen $d > 0.5$). This suggests that VAT explains a part, but not the whole, association between BAT and the metabolic parameters.

It is possible that BAT function affects the degree of visceral adiposity, hence the reciprocal relationship between visceral fat mass and BAT we have shown here could affect metabolic health in severe obesity. Mechanistically, human BAT contributes to diet-induced thermogenesis, resulting in increased oxidation of glucose and lipoprotein-derived fatty acids (30). The postprandial combustion of excess energy by BAT could thus limit visceral fat accumulation and the progression of insulin resistance. Visceral adipose tissue is also a site of deleterious cytokine production, including interleukin 6 (31), levels of which were significantly lower in BAT_{pos} participants in our study (Fig. 4*A* and Supplementary Fig. 4*A*).

BAT Was Linked to Less NAFLD and Lower Metabolic Risk

The more favorable inflammatory state observed in BAT_{pos} participants was also accompanied by reduced signs of NAFLD and hepatic inflammation (Fig. 4). This is in accordance with a previous observation that the presence of BAT was independently associated with a lower likelihood of NAFLD in a large series of ^{18}F-FDG PET/CT images obtained at room temperature (32). The strong correlation between visceral adiposity and NAFLD due to a systemic spillover of lipids and inflammatory cytokines has been widely described (33). Results of recent studies suggest BAT is an endocrine organ that secretes several beneficial adipokines (BATokines), such as FGF-21, neuregulin 4, and bone-morphogenic proteins that can also interact with the liver (34). Hence, it is possible that active BAT might protect against NAFLD via a dual mechanism: the decrease in visceral adiposity and direct BAT effects on the liver potentially mediated through BATokines (35). However, we did not find any association between BAT activity and the putative BATokine FGF-21 in this cohort (Supplementary Fig. 5).

The notion that active BAT may be a crucial determinant of the metabolic risk during obesity gains additional significance in light of a report that was published during the preparation of the present article, which showed that the presence of BAT was associated with a lower prevalence of cardiometabolic diseases in >52,000 patients with cancer (36). In another recent study, active BAT was associated with improved plasma lipid and adiponectin levels in obese individuals, corroborating a potential salutary role in obesity-related metabolic dysregulation (27).

Limitations

One limitation to this study is that our study population was mostly female, because the participants were recruited before bariatric surgery, an intervention more often performed in women. Given that all BAT_{pos} participants were female, no conclusions can be made about the metabolic effects of BAT in obese men. It has been hypothesized that BAT ^{18}F-FDG uptake is merely a marker of BAT insulin sensitivity and thus may not be the ideal radiotracer for quantifying BAT activity (37). Yet, ^{18}F-FDG PET/CT is still considered by many as the gold standard for BAT quantification (22). Moreover, the strong correlation between CIT with BAT ^{18}F-FDG uptake observed in our study and by many others (6,38–40) endorses also a functional association between BAT ^{18}F-FDG uptake and BAT metabolic activity beyond insulin sensitivity. In addition, higher CIT and improved metabolic markers in HOMA-IR–matched BAT_{pos} women (Supplementary Fig. 6 and Supplementary Table 2) also suggest a potential association between BAT activity and metabolic improvements independent of insulin resistance. However, the cross-sectional nature of the study and the small sample size of this subgroup analysis do not allow any firm conclusions about whether active BAT is the cause or the consequence of an advantageous metabolic phenotype in obesity.

During our cooling protocol, we assessed shivering by EMG in the pectoralis major muscle. Because shivering does not occur uniformly, we cannot exclude shivering in other muscles that may have contributed toward CIT. In general, CIT also increases with the degree of thermal

stress. However, both groups had similar cooling-vest temperatures, similar skeletal muscle glucose uptake, and similar cold-induced norepinephrine concentrations, suggesting similar thermal conditions during the cooling procedure.

Conclusion

In summary, we show here that 35% of the individuals with class II-III grade obesity had active BAT. Despite a higher total body fat content, they had a significantly healthier metabolic profile. Specifically, participants with class II-III grade obesity had lower visceral fat mass, less insulin resistance, and better glycemic control, as well as reduced markers of NAFLD, compared with individuals with no detectable BAT ^{18}F-FDG uptake. Our data are in line with a recent report in which the authors support a paradigm shift that active BAT is not negatively associated with adiposity per se (28). BAT seems to be functional in a significant fraction of patients with class II-III obesity and may even contribute toward a metabolically healthy obese phenotype, perhaps through effects on body fat distribution. It is possible to recruit BAT even in states with low basal BAT abundance, such as obesity or diabetes (14,41). Future work should focus on the efficacy of pharmacological BAT activators to recruit BAT in individuals with obesity and, at the same time, evaluate the potential to combat the progression of the metabolic syndrome and its disastrous cardiometabolic sequelae.

Funding. This work was supported by the Austrian Science Fund P 27391, the Medical Scientific Fund of the Mayor of the City of Vienna 17094, and the Austrian Diabetes Association Research Fund, all to F.W.K.

Duality of Interest. No potential conflicts of interest relevant to this article were reported.

Author Contributions. Study conception and design: F.W.K. and O.C.K. conceived the study and its design; C.S., C.T.H., F.B.L., G.P., O.C.K., and M.P. contributed to data collection; A.K.-W., A.R.H., C.S., C.T.H., F.W.K., M.H., M.P., O.C.K., and R.M. contributed to analysis and interpretation of results; C.T.H. drafted the manuscript. All authors reviewed the results and approved the final version of the manuscript. F.W.K. is the guarantor of this work and, as such, had full access to all the data in the study and takes responsibility for the integrity of the data and the accuracy of the data analysis.

References

1. Abdelaal M, le Roux CW, Docherty NG. Morbidity and mortality associated with obesity. Ann Transl Med 2017;5:1–12

2. Goossens GH. The metabolic phenotype in obesity: fat mass, body fat distribution, and adipose tissue function. Obes Facts 2017;10:207–215

3. Roberson LL, Aneni EC, Maziak W, et al. Beyond BMI: the "metabolically healthy obese" phenotype & its association with clinical/subclinical cardiovascular disease and all-cause mortality–a systematic review. BMC Public Health 2014;14:1–12

4. van Marken Lichtenbelt WD, Vanhommerig JW, Smulders NM, et al. Cold-activated brown adipose tissue in healthy men. N Engl J Med 2009;360:1500–1508

5. Virtanen KA, Lidell ME, Orava J, et al. Functional brown adipose tissue in healthy adults. N Engl J Med 2009;360:1518–1525

6. Saito M, Okamatsu-Ogura Y, Matsushita M, et al. High incidence of metabolically active brown adipose tissue in healthy adult humans: effects of cold exposure and adiposity. Diabetes 2009;58:1526–1531

7. Orava J, Nuutila P, Noponen T, et al. Blunted metabolic responses to cold and insulin stimulation in brown adipose tissue of obese humans. Obesity (Silver Spring) 2013;21:2279–2287

8. Yoneshiro T, Aita S, Matsushita M, et al. Recruited brown adipose tissue as an antiobesity agent in humans. J Clin Invest 2013;123:3404–3408

9. Cannon B, Nedergaard J. Brown adipose tissue: function and physiological significance. Physiol Rev 2004;84:277–359

10. Yoneshiro T, Aita S, Matsushita M, et al. Brown adipose tissue, whole-body energy expenditure, and thermogenesis in healthy adult men. Obesity (Silver Spring) 2011;19:13–16

11. Kulterer OC, Niederstaetter L, Herz CT, et al. The presence of active brown adipose tissue determines cold-induced energy expenditure and oxylipin profiles in humans. J Clin Endocrinol Metab 2020;105:2203–2216

12. Yoneshiro T, Aita S, Matsushita M, et al. Age-related decrease in cold-activated brown adipose tissue and accumulation of body fat in healthy humans. Obesity (Silver Spring) 2011;19:1755–1760

13. van der Lans AAJJ, Hoeks J, Brans B, et al. Cold acclimation recruits human brown fat and increases nonshivering thermogenesis. J Clin Invest 2013;123:3395–3403

14. Hanssen MJW, Hoeks J, Brans B, et al. Short-term cold acclimation improves insulin sensitivity in patients with type 2 diabetes mellitus. Nat Med 2015;21:863–865

15. Das SK, Roberts SB, Kehayias JJ, et al. Body composition assessment in extreme obesity and after massive weight loss induced by gastric bypass surgery. Am J Physiol Endocrinol Metab 2003;284:E1080–E1088

16. Bosy-Westphal A, Schautz B, Later W, Kehayias JJ, Gallagher D, Müller MJ. What makes a BIA equation unique? Validity of eight-electrode multifrequency BIA to estimate body composition in a healthy adult population. Eur J Clin Nutr 2013;67(Suppl. 1):S14–S21

17. Borges JH, Guerra-Júnior G, Gonçalves EM. Methods for data analysis of resting energy expenditure measured using indirect calorimetry. Nutrition 2019;59:44–49

18. Otgonsuren M, Estep MJ, Hossain N, et al. Single non-invasive model to diagnose non-alcoholic fatty liver disease (NAFLD) and non-alcoholic steatohepatitis (NASH). J Gastroenterol Hepatol 2014;29:2006–2013

19. Matthews DR, Hosker JP, Rudenski AS, Naylor BA, Treacher DF, Turner RC. Homeostasis model assessment: insulin resistance and beta-cell function from fasting plasma glucose and insulin concentrations in man. Diabetologia 1985;28:412–419

20. Matsuda M, DeFronzo RA. Insulin sensitivity indices obtained from oral glucose tolerance testing: comparison with the euglycemic insulin clamp. Diabetes Care 1999;22:1462–1470

21. American Diabetes Association. 2. Classification and diagnosis of diabetes: *Standards of Medical Care in Diabetes-2020*. Diabetes Care 2020;43(Suppl. 1):S14–S31

22. Chen KY, Cypess AM, Laughlin MR, et al. Brown Adipose Reporting Criteria in Imaging STudies (BARCIST 1.0): recommendations for standardized FDG-PET/CT experiments in humans. Cell Metab 2016;24:210–222

23. Iwen KA, Backhaus J, Cassens M, et al. Cold-induced brown adipose tissue activity alters plasma fatty acids and improves glucose metabolism in men. J Clin Endocrinol Metab 2017;102:4226–4234

24. Keramida G, Potts J, Bush J, Verma S, Dizdarevic S, Peters AM. Accumulation of (^{18})F-FDG in the liver in hepatic steatosis. AJR Am J Roentgenol 2014;203:643–648

25. Staiger H, Keuper M, Berti L, Hrabe de Angelis M, Häring H-U. Fibroblast growth factor 21—metabolic role in mice and men. Endocr Rev 2017;38:468–488

26. Vijgen GHEJ, Bouvy ND, Teule GJJ, Brans B, Schrauwen P, van Marken Lichtenbelt WD. Brown adipose tissue in morbidly obese subjects. PLoS One 2011;6:e17247

27. Mihalopoulos NL, Yap JT, Beardmore B, Holubkov R, Nanjee MN, Hoffman JM. Cold-activated brown adipose tissue is associated with less cardiometabolic dysfunction in young adults with obesity. Obesity (Silver Spring) 2020;28:916–923
28. Sanchez-Delgado G, Martinez-Tellez B, Acosta FM, et al. Brown adipose tissue volume and fat content are positively associated with whole-body adiposity in young men—not in women. Diabetes 2021;70:1473–1485
29. Martinez-Tellez B, Sanchez-Delgado G, Garcia-Rivero Y, et al. A new personalized cooling protocol to activate brown adipose tissue in young adults. Front Physiol 2017;8:1–10
30. U Din M, Saari T, Raiko J, et al. Postprandial oxidative metabolism of human brown fat indicates thermogenesis. Cell Metab 2018;28:207–216.e3.
31. Trayhurn P. Hypoxia and adipose tissue function and dysfunction in obesity. Physiol Rev 2013;93:1–21
32. Yilmaz Y, Ones T, Purnak T, et al. Association between the presence of brown adipose tissue and non-alcoholic fatty liver disease in adult humans. Aliment Pharmacol Ther 2011;34:318–323
33. Stefan N, Häring H-U, Cusi K. Non-alcoholic fatty liver disease: causes, diagnosis, cardiometabolic consequences, and treatment strategies. Lancet Diabetes Endocrinol 2019;7:313–324
34. Villarroya F, Cereijo R, Villarroya J, Giralt M. Brown adipose tissue as a secretory organ. Nat Rev Endocrinol 2017;13:26–35
35. Scheja L, Heeren J. Metabolic interplay between white, beige, brown adipocytes and the liver. J Hepatol 2016;64:1176–1186
36. Becher T, Palanisamy S, Kramer DJ, et al. Brown adipose tissue is associated with cardiometabolic health. Nat Med 2021;27:58–65
37. Richard MA, Pallubinsky H, Blondin DP. Functional characterization of human brown adipose tissue metabolism. Biochem J 2020;477:1261–1286
38. Chen KY, Brychta RJ, Linderman JD, et al. Brown fat activation mediates cold-induced thermogenesis in adult humans in response to a mild decrease in ambient temperature. J Clin Endocrinol Metab 2013;98:E1218–E1223
39. Hanssen MJW, Wierts R, Hoeks J, et al. Glucose uptake in human brown adipose tissue is impaired upon fasting-induced insulin resistance. Diabetologia 2015;58:586–595
40. Fischer JGW, Maushart CI, Becker AS, et al. Comparison of [^{18}F]FDG PET/CT with magnetic resonance imaging for the assessment of human brown adipose tissue activity. EJNMMI Res 2020;10:1–12
41. Hanssen MJW, van der Lans AAJJ, Brans B, et al. Short-term cold acclimation recruits brown adipose tissue in obese humans. Diabetes 2016;65:1179–1189